



Mathematical model for the analysis of structure and optimal operational parameters of a solid oxide fuel cell generator



Alberto Coralli ^{a, b,*}, Hugo Villela de Miranda ^a, Carlos Felipe Espiúca Monteiro ^a, José Francisco Resende da Silva ^c, Paulo Emílio Valadão de Miranda ^b

^a EnergiaH, Avenida das Américas 4319, Room 204, Barra da Tijuca, 22631-004 Rio de Janeiro, RJ, Brazil

^b Hydrogen Laboratory, COPPE, Federal University of Rio de Janeiro, Avenida Horácio Macedo 2030, Room I-146, Ilha do Fundão, 21941-914 Rio de Janeiro, RJ, Brazil

^c Elektro, Rua Ary Antenor de Souza 321, Jardim Nova América, 13053-024 Campinas, SP, Brazil

HIGHLIGHTS

- Potential markets for ethanol-fueled solid oxide fuel cell power systems in Brazil are analyzed.
- A simulation model of this kind of power system is formulated.
- The model is run with different system configurations to identify the optimal one.
- Operation with pure ethanol or, in alternative, with anodic recirculation proves to be the best operating conditions.

ARTICLE INFO

Article history:

Received 14 February 2014

Received in revised form

27 June 2014

Accepted 30 June 2014

Available online 8 July 2014

Keywords:

Balance of plant

Ethanol

Brazil

Mathematical model

Solid oxide fuel cell

ABSTRACT

Solid oxide fuel cells are globally recognized as a very promising technology in the area of highly efficient electricity generation with a low environmental impact. This technology can be advantageously implemented in many situations in Brazil and it is well suited to the use of ethanol as a primary energy source, an important feature given the highly developed Brazilian ethanol industry. In this perspective, a simplified mathematical model is developed for a fuel cell and its balance of plant, in order to identify the optimal system structure and the most convenient values for the operational parameters, with the aim of maximizing the global electric efficiency. In this way it is discovered the best operational configuration for the desired application, which is the distributed generation in the concession area of the electricity distribution company Elektro. The data regarding this configuration are required for the continuation of the research project, i.e. the development of a prototype, a cost analysis of the developed system and a detailed perspective of the market opportunities in Brazil.

© 2014 Elsevier B.V. All rights reserved.

1. Introduction

The field of new energy converters has recently been the target of intense research activities, with the main goal of improving systems' energy efficiency, while facing the challenges related pollutant emissions reduction. In this scenario, one of the most promising technologies is the Fuel Cell (FC). Fuel cells are electric

energy generators characterized by their high efficiency (about 50% based on the net energy produced [1]) and very low pollutant emissions. The electric energy generation results from direct conversion of the fuel's chemical energy through electrochemical reactions. In addition to the fuel cells themselves, arranged in stacks, electric generation systems based on FCs require various auxiliary devices, collectively called Balance of Plant (BoP) of the fuel cell stack.

One type of FC that attracts great interest in the scientific community is the Solid Oxide Fuel Cell (SOFC), which uses a solid ceramic electrolyte capable of conducting oxygen ions (O^{2-}) from the cathode to the anode [1]. The operating temperature varies between 650 °C and 1000 °C. The fuel can be hydrogen, biogas or simple hydrocarbons, which can decompose to CO and H₂ inside the SOFC anode, or synthesis gas obtained through previous

* Corresponding author. Hydrogen Laboratory, COPPE, Federal University of Rio de Janeiro, Avenida Horácio Macedo, 2030, sala I-146, Ilha do Fundão, 21941-914 Rio de Janeiro, RJ, Brazil. Tel.: +55 21 25628791.

E-mail addresses: alberto.coralli@energiah.com.br, alberto.coralli@labh2.coppe.ufrj.br (A. Coralli), hmiranda@energiah.com.br (H. Villela de Miranda), carlos@energiah.com.br (C.F. Espiúca Monteiro), jose.resende@elektro.com.br (J.F. Resende da Silva), pmiranda@labh2.coppe.ufrj.br (P.E. Valadão de Miranda).

chemical treatment of complex hydrocarbons. Two important advantages of this kind of FC are the capacity to work with fuels other than pure hydrogen and the high temperature of the heat generated as a byproduct of the electric energy production. Due to their peculiar characteristics, SOFCs are particularly well suited to use in high efficiency stationary Combined Heat and Power (CHP) systems, with power ranging from 500 W up to several MW. In fact, the energetic performance of fuel cell based generation systems is approximately a constant function of the produced power.

One of the most interesting applications of low power SOFCs is in micro-CHPs (combined heat and electric power generators characterized by nominal electric power lower than 50 kW, according to the European Union's definition [2]). This is a technological area where relevant development efforts are concentrated, particularly aiming to obtain more efficient, sustainable and stable national electric generation grids, by means of the widespread use of high efficiency micro-CHP units in a distributed generation scheme, as evidenced in the literature [3]. However, to reach a true beneficial effect, it is vitally important that these micro-CHP units have an efficiency similar to that observed in modern centralized generation systems. This requirement cannot be easily satisfied using conventional technologies, but it can be reached using FC systems, which present high efficiencies even when working at low power levels. As a consequence, fuel cell systems are potential candidates for massive diffusion of micro-CHP systems. In this area, SOFC technology seems to be particularly promising [4], offering the previously mentioned advantages over other types of FCs. During the last ten years, the research in this field has been intense, leading to the creation of several prototypes and pre-commercial products. Several installation programs were initiated in order to demonstrate the technology [5,6], and some companies are in the first commercialization stage of SOFC-based methane-fueled micro-CHPs, introduced in the market as substitutes for the traditional domestic heaters, widely used for residential applications. Given the proposed application, these devices are usually designed in a way to maximize global efficiency (sum of thermal and electrical efficiencies) and to assure enough thermal power, treating the electric energy just like a useful byproduct of heat production.

2. Potential markets in Brazil

In Brazil, energy generation and its use have peculiar profiles, very different from the ones that characterize most other economically important countries on the global scale. One important characteristic is the high percentage of electric energy that is produced through renewable sources (89%), mainly hydropower and biomass, with a small wind power contribution [7]. Another important aspect is the minimal use of energy for residential heating, limited to small areas of the country and only for few days a year. Moreover, the country presents the need for a considerable expansion of the energy production, transmission and distribution infrastructure, to support the country's economic growth and extend the availability of electrical power in remote areas. To tackle this last issue, a federal program was launched: between 2003 and 2013 more than 3 million new electric connections were implemented, with an investment of R\$ 20 billion [8]. Despite this investment, some areas of the country still lack a connection to the national transmission grid, and a substantial growth of demand is expected. Therefore, it is probable that the country's power supply needs will grow even more in the next years, requiring additional grid reinforcement or alternative solutions such as distributed generation. Finally, Brazil possesses an important bioethanol production capacity and distribution infrastructure [7], well established in every Brazilian state, including both large industries and small family-operated agro-industries. The primary energy

generation from sugar cane products showed steep growth in the last years and in 2009 surpassed the hydroelectric energy generation in the country.

Given this scenario, the use of SOFC micro-CHP systems would also present some peculiarities, such as the use of ethanol as fuel, instead of methane, and the operation essentially dedicated to electric production, even though some areas of the country present periods of cold weather, when the residential cogeneration of electricity and heat could be interesting. There are many situations in Brazil where the use of SOFC systems could bring environmental and economic benefits. A first application is the substitution of generators characterized by high environmental impact (in most cases internal combustion engines). These are currently used in some specific cases, including the generation of power when the electric energy reaches its peak in demand (and as a consequence the cost is higher), or the supply of electricity to remote places not connected to the national transmission grid, or even the strengthening of load covering capacities in small groups of grid users distant from the main company grid that do not present a regular consumption high enough to justify the installation of new higher capacity cables. It would be possible to replace the above mentioned generators with SOFC systems, maintaining the same service and infrastructure quality, but markedly increasing generation efficiency and at the same time reducing pollutant emissions. The Brazilian market for peak-hour additional generation capacity is estimated to lie between 3 and 10 GW [9]. Until recently, the energy generated to meet this peak-hour demand was produced through the use of internal combustion engines, but an increase in the price of diesel and a drop in the electricity peak price have made this solution less economically viable. On the other hand, ethanol-fueled SOFC systems could offer better economic performance, due to this type of equipment's higher electric efficiency. Furthermore, the electric energy demand projected for the next years can be used to evaluate the potential market size for distributed generation. The expected increase in Brazilian electricity demand between 2012 and 2022 has been estimated around 275 TWh, including grid supplied power and autoproduction (industrial cogeneration and distributed generation) [10]. This value represents an increase of approximately 55% with respect to the current figures. Admitting that a large part of this considerable demand increase will be satisfied using conventional methods (namely, expansion of centralized generation and power transmission grids), the potential market for distributed generation in Brazil is still very important, especially considering that the size of the country implies high costs of transmission lines. For example, the current cost of a 345 kV line can be evaluated around 584,000 R\$ km⁻¹ [11]. As a consequence, in several cases the cost of the lines required to connect remote locations to the national transmission grid, or to increase the power capacity of existing connections, can make the dissemination of distributed generators with higher cost per installed kW economically viable. In this scenario, ethanol-fueled SOFC micro-CHPs could offer unique advantages over other technologies, namely the possibility to generate energy on demand using a renewable energy source. In addition to what was stated up to now in this section, it should be noted that, even though centralized electric generation in Brazil basically relies on renewable sources, its environmental impact is not negligible. Being mostly of hydro-electrical origin, it involves a considerable production of methane and carbon dioxide from organic material decomposition in water reservoirs [12]; in fact, the extension of water accumulation lakes can be used to quantify the environmental impact of these plants [13]. Moreover, since it is centralized, this kind of generation requires a big transmission and distribution infrastructure that presents high financial and environmental costs, and creates relevant losses in efficiency. As a consequence, the use

of SOFC-based micro-CHPs fueled by bioethanol in a distributed generation pattern supplying base power to the grid could represent a practical way of generating additional renewable electricity with a reduced environmental impact.

Given the situation described, a research project was initiated, aiming at the development of a hybrid system based on an ethanol-fueled SOFC and with the main objective of generating electric energy in the micro-CHP power range. The term "hybrid" means that the SOFC should produce a constant net power of 500 W, as part of a more complex system that also includes a battery pack used to compensate for the electric load variations, thereby maintaining the fuel cell power output essentially constant. In this way, it is possible to reduce the power transients the fuel cell needs to sustain, increasing its life span [14]. In fact, frequent variations in the fuel cells' operational conditions can lead to accelerate performance degradation [15]. Another important characteristic of the system will be the direct use of ethanol, without previous chemical processing. This will be possible with the use of a recently developed anode material for SOFC fabrication [16,17] which possesses electrocatalytic action for the direct oxidation of ethanol without solid carbon formation inside the fuel cells. Also the BoP structure, materials and management strategy contribute in avoiding carbon deposition problems. This characteristic will be an important difference with respect to other existing prototypes, where the fuel goes through a series of chemical treatments before entering the fuel cell stack. The application of these treatments would imply the use of one or more additional reactors that increase the cost and the complexity of the system.

The first step of the research consisted in conceiving a simplified mathematical model of the SOFC-BoP ensemble (excluding the batteries and the interface generator/grid) and using it to evaluate some possible system construction topologies, looking for the optimal values of the operational parameters in each different case. The data obtained will be used in the further steps of the research to fix the specifications of the system and to build an experimental prototype. The applied model is purely thermodynamic, not containing any economic consideration about the cost of the system.

3. Mathematical model

The system's mathematical model includes the main components that have been proposed for use in the construction of the SOFC-BoP ensemble prototype. The list of components was created through basic project activity of the system and comparison with some structures described in the literature ([18,19]). Some of the chosen components (labeled as "optional") are not present in all the versions that were considered as alternatives for system fabrication:

- ethanol pump, used to feed fuel to the stack;
- ethanol tank;
- water pump (optional), can be employed to create a water flow, used to prevent the formation and the deposition of solid carbon in the system's pipes and inside the SOFC;
- water tank (optional);
- blower, used to generate the air flow needed for fuel cell reactions;
- after-burner, a combustor where the excess fuel which did not react in the SOFC burns completely;
- fuel and air pre-heating heat exchangers;
- recirculation ejectors (optional), used to promote a partial recirculation of anode and cathode outlet gases to the anodic and cathodic inlets respectively. In the ejectors, the fuel (or air) flow created by the ethanol pump (or the air blower) transfers part of its momentum to a portion of the flow that exits from the

anode (or the cathode), generating the recirculation of a portion of the gas, which reenters the SOFC;

- power electronic device, properly conditions the electric power produced by the fuel cell;
- heat recovery heat exchanger, uses the residual energy content of after-burner outlet gases to heat a flow of water.

Fig. 1 shows the basic layout; numeric indeces are used in the model description to indicate different system points.

The modeled generation system has the main goal of producing electric energy at constant power, while a battery bank, not included in the model, compensates for load power fluctuations. As a consequence, in this stage of the development the model describes only the stationary system regime.

3.1. SOFC model

The electricity generation device of the system is a SOFC stack, an electrochemical equipment capable of converting ethanol's chemical energy directly into electric energy. Actually, ethanol is decomposed in simpler compounds through different reactions before it reaches the FC anode. The result of these reactions is the production of hydrogen, water, carbon monoxide and carbon dioxide. The elements that take part in the electrochemical reactions are essentially carbon monoxide and hydrogen in the anode, (1) and (2), and oxygen in the cathode, (3):



In this model, it is assumed that all ethanol is converted to CO and H₂ inside fuel cells anodic compartments or in gas feeding pipes, before reaching the active sites where the chemical reactions take place. This result can be obtained in a real system through different strategies [20]:

- external reforming – the fuel, together with steam, goes through a reactor that contains a catalyst capable of promoting reactions that break down the ethanol molecule. Common reactions are called steam reforming (4) and water–gas shift (5):



The first reaction requires high temperatures and is strongly endothermic; the second is mildly exothermic. This means that generally it is necessary to supply heat to the reactor in order to maintain its thermal equilibrium. Hence, the presence of this external reactor considerably complicates the system's construction and control, increasing its cost. Due to these considerations, the described project focuses on the research of solutions that do not involve external reforming. Therefore, this option was not included in the alternatives explored by the model;

- internal reforming – ethanol is fed directly to the SOFC blended with steam. In this case there is no dedicated reforming reactor: (4) and (5) happen in the anodic compartments. In this way, it is possible to obtain an optimal thermal balance between the heat produced by the electrochemical reactions (1)–(3), exothermic

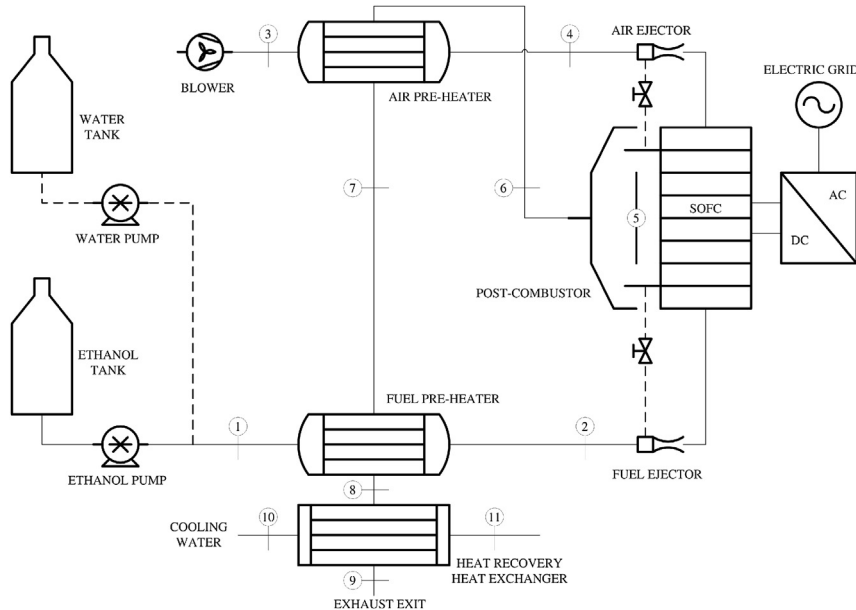


Fig. 1. Basic layout of SOFC-BoP ensemble. In the scheme, all the components listed in this section are represented, together with the connections between them. Dashed lines indicate optional piping connections.

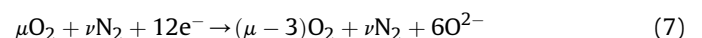
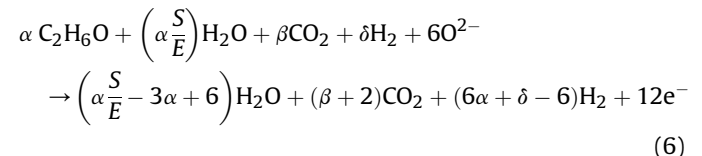
reactions, and the heat required by the steam reforming (4). The resulting system is simpler and cheaper than in the previous case, but it still needs a steam source. The viability of this option was explored in the literature [21]:

- direct utilization – the SOFC stack is fed with pure ethanol, without any steam addition. However, the ethanol molecule is ripped apart by pyrolysis reactions before reaching the interior of the porous matrix of the anode, producing simpler compounds that can react at the active sites that exist in the region of the anode where the electrochemical reaction takes place. When the stack reaches the steady state, water produced by the oxidation of hydrogen (1) is present at the anode. Therefore, in this condition, reactions (4) and (5) can happen, even though no steam is being added from outside the stack (as verified in Ref. [22]). This solution guarantees lower system complexity. On the other hand, when a SOFC stack is operated in this way there is generally a possibility of solid carbon formation inside the stack and the high temperature pipes. The components of the system which are potentially affected by soot formation are the parts of the fuel inlet pipes where the temperature is high enough to favor fuel pyrolysis reactions, the fuel inlet manifold of the stack and the anode compartments of the fuel cells. Moreover, pyrolysis reactions can be favored by the contact between the fuel and some elements or compounds, which can act as catalysts and lower the temperature range in which solid carbon formation is considerable. As a consequence, a possible way to eliminate this problem is the use of materials that do not favor or avoid carbon deposition. In the present paper, it is assumed that the use of an innovative material ([16, 17]), already mentioned in Section 2, and the BoP structure, materials and management strategy make it possible to obtain the optimal situation in which there is no carbon deposition, neither in the stack nor in other parts of the system.

The present model considers only the system's steady state condition. In this situation, the SOFC anode contains water also in the case of the direct utilization of ethanol. For simplicity, the model is applied only with the combinations of operational parameters that guarantee that the amount of water in the stack anodes is enough to convert through reaction (4) all of the ethanol

supplied. In addition to that, in normal operating conditions reaction (5) happens approximately four times faster than (2) [23]. As a consequence, in this model the water–gas shift reaction is considered as the only mechanism capable of consuming carbon monoxide (electrochemical oxidation is neglected). The global result of (1)–(5) is therefore ethanol conversion to CO₂ and H₂ with subsequent electrochemical oxidation of the hydrogen produced. The magnitude of the errors introduced with these hypotheses will be quantified in the subsequent steps of the research.

The model is built assuming that (1)–(5) happen at the same time and that all carbon contained in the ethanol reacts, forming carbon dioxide. In this way, it is possible to write global reactions, also considering the possibility of partial recirculation of reaction products between anode and cathode inlets and outlets. The formulas were obtained applying (4) and (5) for all ethanol supplied, and (1)–(3) only for the amount allowed by transferred oxygen ions. Both anodic (6) and cathodic (7) reactions were written using as calculation basis six of the oxygen ions among those transferred from the cathode to the anode through the electrolyte:



where S/E is the ratio between the number of moles of steam and ethanol entering the stack. α , β , δ , μ and ν are the stoichiometric coefficients of ethanol, carbon dioxide, hydrogen, oxygen and nitrogen, respectively. To calculate these coefficients, a balance of available electrons at the anodic inlet was used:

$$12\alpha + 2\delta = 12\lambda_{fuel} \quad (8)$$

λ_{fuel} indicates the ratio between the amount of fuel supplied and the stoichiometric amount, which is the minimal amount of fuel

required to complete the reactions with the oxygen ions. λ_{fuel} is the inverse of the fuel utilization rate, another parameter widely used in the literature. An additional relation is introduced to allow for the calculation of the stoichiometric coefficients and is written considering that the anodic recycling fraction $f_{\text{REC},A}$, defined as the ratio between the amount of a chemical compound entering the anode as a result of recirculation and the amount of the same compound leaving the anode, is the same for all compounds that are not introduced from outside the stack:

$$f_{\text{REC},A} = \frac{\delta}{6\alpha + \delta - 6} = \frac{\beta}{\beta + 2} = \frac{\alpha \cdot \frac{S}{E} \cdot (1 - f_{\text{H}_2\text{O},e})}{\alpha \cdot \frac{S}{E} - 3\alpha + 6} \quad (9)$$

This is not valid for the substances that are introduced from outside the stack (ethanol, water, oxygen and nitrogen), since in this case it is necessary to include also the external flow in the mass balance. Two additional project parameters are used to determine the values related to these compounds as well: the fraction of water flow introduced from outside the stack, $f_{\text{H}_2\text{O}}$, and the cathodic recirculation fraction $f_{\text{REC},C}$. This last parameter, defined in the same way as $f_{\text{REC},A}$, can also be used to evaluate the fraction of oxygen that is introduced from outside the stack:

$$f_{\text{O}_2,e} = \frac{\dot{n}_{\text{O}_2,e}}{\dot{n}_{\text{O}_2,\text{in}}} = 1 - \frac{\mu - 3}{\mu} \cdot f_{\text{REC},C} \quad (10)$$

which is the ratio between the molar flow rate of oxygen introduced in the stack from outside $\dot{n}_{\text{O}_2,e}$ and the total molar flow rate of oxygen entering the cathode compartments $\dot{n}_{\text{O}_2,\text{in}}$. In addition, it is assumed that the cathodic fluid is air (this implies that approximately 3.76 mol of nitrogen are introduced in the stack for every mole of oxygen). Finally, it is possible to introduce the parameter λ_{O_2} , analogous to λ_{fuel} , which indicates the ratio between the amount of oxygen actually supplied and the stoichiometric amount, which is the minimal amount of oxygen required to complete the reactions with the electrons coming from the anode through the electrolyte. From reaction (7), it can be concluded that λ_{O_2} can be expressed as in equation (11):

$$\lambda_{\text{O}_2} = \frac{\mu}{3} \quad (11)$$

The stoichiometric coefficients introduced in (6) and (7) give the molar fractions of all chemical substances contained in the gas flow exiting from the stack, according to following relation:

$$x_i = \frac{C_i}{\sum_j C_j} \quad (12)$$

C_i and C_j are the stoichiometric coefficients of compounds i and j , and the sum is extended to all compounds that are present in the outlet flow. After determining the reactions' stoichiometry, the Nernst equation was used in order to define the theoretical open circuit voltage for each single cell:

$$E_N = -\frac{\Delta G^0}{n \cdot F} - \frac{R \cdot T_S}{n \cdot F} \cdot \ln \left(\frac{x_{\text{H}_2\text{O}}}{x_{\text{H}_2} \cdot x_{\text{O}_2}^{1/2}} \right) \quad (13)$$

An explanation of each term can be found in common fuel cell literature [1]. When a load is applied, this maximum voltage level is reduced due to ohmic and activation losses, as indicated in equation (14) (concentration losses are neglected, assuming that the stack does not work close to maximum current condition):

$$V_c = E_N - i \cdot R_c - a - b \cdot \ln(i) \quad (14)$$

with V_c single cell voltage, i current density in A cm⁻², R_c ohmic resistance, a and b constants related to the activation losses. R_c , a and b are calculated as a function of temperature through empirical expressions found in the literature for the case of a typical solid oxide cell [23]. If N_c and A_c are respectively the number of cells in the stack and the active area of a single cell, the electric power produced can be expressed by:

$$P_{\text{el,SOFC}} = V \cdot I = N_c \cdot V_c \cdot i \cdot A_c \quad (15)$$

V_c and i are calculated fixing N_c , A_c and P_{el} as project data. The required molar flow rate of ethanol is related to the total current I (product of current density and cell's active area) through the following equation that is obtained considering the electronic balance (8) and the reaction (6):

$$\dot{n}_{\text{C}_2\text{H}_6\text{O}} = \frac{I \cdot N_c \cdot \alpha}{12F} \quad (16)$$

The molar flow rates of the other compounds present in the anode inlet and outlet flows are calculated according to the stoichiometry indicated in (6), using the generic relation (17):

$$\dot{n}_i = \dot{n}_{\text{C}_2\text{H}_6\text{O}} \cdot \frac{C_i}{C_{\text{C}_2\text{H}_6\text{O}}} = \dot{n}_{\text{C}_2\text{H}_6\text{O}} \cdot \frac{C_i}{\alpha} \quad (17)$$

where $C_{\text{C}_2\text{H}_6\text{O}}$ is the stoichiometric coefficient of ethanol (equal to α) and C_i is the stoichiometric coefficient of the chemical specie i , related to the inlet or outlet molar flow rate n_i of the chemical specie i . In a similar way, the molar flow rate of oxygen introduced in the stack from outside can be calculated using equation (18), analogous to equation (16):

$$\dot{n}_{\text{O}_2,e} = \frac{I \cdot N_c}{4F} \cdot [\lambda_{\text{O}_2} - f_{\text{REC},C} \cdot (\lambda_{\text{O}_2} - 1)] \quad (18)$$

and the molar flow rate of nitrogen introduced in the stack from outside is calculated in equation (19) taking into account the definition of $f_{\text{O}_2,e}$ expressed by equation (10):

$$\dot{n}_{\text{N}_2,e} = 3.76 \cdot \dot{n}_{\text{O}_2,e} = 3.76 \cdot f_{\text{O}_2,e} \cdot \dot{n}_{\text{O}_2,\text{in}} \quad (19)$$

The total chemical power introduced in the SOFC through the fuel flow results from the relation:

$$P_{\text{tot}} = -\Delta H_{\text{C}_2\text{H}_6\text{O}} \cdot \dot{n}_{\text{C}_2\text{H}_6\text{O}} \quad (20)$$

where $\Delta H_{\text{C}_2\text{H}_6\text{O}}$ is ethanol's enthalpy of combustion. The stack's electric efficiency is:

$$\eta_{\text{el,SOFC}} = \frac{P_{\text{el,SOFC}}}{P_{\text{tot}}} \quad (21)$$

As previously stated, in the stack each mole of ethanol reacts with steam according to (4) and (5), and part of the produced hydrogen reacts in (1). It is also necessary to include in the model the effects of the reactions over SOFC's thermal balance. By introducing hydrogen's enthalpy of combustion ΔH_{H_2} , the sum of the enthalpies of reaction associated with steam reforming and water gas shift reactions ΔH_{sr} , and the thermal power absorbed by the gases circulating in the cells through convection Q_{conv} , it is possible to obtain the thermal power that is produced by the stack using the following energy balance:

$$Q_{SOFC} = -\Delta H_{C_2H_6O} \cdot \dot{n}_{C_2H_6O} + \Delta H_{H_2} \cdot \dot{n}_{H_2} - P_{el} - \Delta H_{sr} \cdot \dot{n}_{C_2H_6O} - Q_{conv} \quad (22)$$

where \dot{n}_{H_2} is hydrogen flow at SOFC outlet. If the thermal powers associated with anode and cathode inlet gas flows are indicated with Q_2 and Q_4 , the sum of the outlet flows thermal powers is:

$$Q_5 = Q_2 + Q_4 + Q_{conv} \quad (23)$$

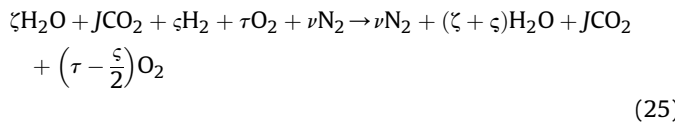
An estimate of the convective thermal transfer coefficients in SOFC cells channels [24] shows that the thermal exchange is efficient enough to increase the temperature of the outlet gases to the same level as that of the solid components of the stack. Inlet temperatures are project parameters. Knowing all molar flows, it is possible to calculate the heat flows using the equation:

$$Q_k = T_k \cdot \left(\sum_j c_{p,j}(T_k) \cdot \dot{n}_{j,k} \right) \quad (24)$$

where k indicates the considered position, and the sum is extended to all present chemical compounds. $c_{p,j}(T_k)$ indicates the specific heat at constant pressure of compound j at temperature T_k .

3.2. After-burner model

In order to increase the thermal energy content of SOFC outlet gases and to avoid the emission in the environment of harmful substances like carbon monoxide, the use of an after-burner was considered. In this component, placed after the stack, residual inflammable gases burn according to the equation:



where ζ , ϑ , ϑ , τ , ν are the stoichiometric coefficients of the different substances. Formula (25) was written under the assumption that the oxygen that feeds the SOFC is enough to sustain the electrochemical reaction and completely burns the portion of the fuel that does not react in the cells. Using the stoichiometric coefficients and knowing the composition of the after-burner inlet flow, it is possible to calculate the molar flows of the chemical compounds leaving the after-burner. The total molar flow of the outlet gases n_s is the sum of these flows. Since power Q_{SOFC} may be a negative value (which means that the SOFC requires thermal energy in order to maintain its thermal equilibrium), it is assumed that the after-burner is in direct thermal contact with the stack, exchanging heat flow Q_{SOFC} . In this way, the SOFC internal temperature is considered the same for every simulated condition. Indicating with Q_6 and $Q_{d,AB}$ the thermal power associated with the after-burner outlet gases and the thermal power that is dispersed through the perimeter of the after-burner respectively, it is possible to formulate the following energy balance:

$$Q_6 = Q_5 - \Delta H_{H_2} \cdot \dot{n}_{H_2} - Q_{d,AB} + Q_{SOFC} \quad (26)$$

This balance allows for the evaluation of the temperature of the outlet gases T_6 using equation (24). The mean specific heat of the outlet gas mixture at constant pressure is defined as:

$$\bar{c}_{p,s}(T_6) = \frac{\sum_j c_{p,j}(T_6) \cdot \dot{n}_{j,6}}{\dot{n}_s} \quad (27)$$

where j indicates each chemical compound contained in the outlet gas mixture.

3.3. Blower and pumps models

The power consumed by the fuel pump (and eventually by the water pump) can be expressed as a function of the molar flow of the fluid, the specific enthalpy variation between pump inlet and outlet Δh_f , and the isentropic efficiency of the machine η_p . Alternatively, the same quantity can be represented using the volumetric flow V_f and the pressure variation Δp_f (the temperature variation in a pump is negligible):

$$P_p = \frac{\dot{n}_f \cdot \Delta h_f}{\eta_p} = \frac{\dot{V}_f \cdot \Delta p_f}{\eta_p} \quad (28)$$

An analogous equation can be developed for the power consumed by the air blower [14]. It is possible to express the blower outlet flow temperature for an isentropic compression process using the following equation:

$$T_{3,isentropic} = T_{amb} \cdot \left(\frac{p_o}{p_{amb}} \right)^{\frac{\gamma-1}{\gamma}} \quad (29)$$

As a consequence, the power consumed by the blower can be expressed as:

$$P_b = \frac{\dot{n}_{air} \cdot \Delta h_b}{\eta_b} = \frac{\dot{n}_{air} \cdot c_{air}(T_{amb}) \cdot T_{amb}}{\eta_b} \cdot \left[\left(\frac{p_o}{p_{amb}} \right)^{\frac{\gamma-1}{\gamma}} - 1 \right] \quad (30)$$

where η_b is the blower's isentropic efficiency, p_o is the blower's outlet pressure and γ is the adiabatic expansion coefficient.

To execute the calculations, the isentropic efficiency η_b was considered equal to 0.7 and the pressure drops in the various components were fixed according to Table 1.

3.4. Heat exchangers model

The basic layout of the system includes three heat exchangers, used to recover part of the energy content of the outlet gases, pre-heating the fluids that are fed to the stack and heating a water flow, which can be used by an external user. The following energy balance can be applied to each heat exchanger:

$$Q_{h,i} - Q_{h,o} + Q_{h,vap} = Q_{c,o} - Q_{c,i} + Q_{d,TR} + Q_{c,vap} \quad (31)$$

In equation (31), the heat flows related to the hot fluid and to the cold fluid are indicated, respectively, with subscripts h and c , while subscripts i and o indicate the heat exchanger's inlet and outlet flows. $Q_{d,TR}$ is the thermal power dispersed through the heat exchanger's insulation. $Q_{h,vap}$ and $Q_{c,vap}$ are the latent heats of vaporization of hot and cold fluid, thermal powers that have to be removed or supplied in order to condensate the hot fluid or vaporize the cold fluid. Applying this balance with equation (24), it is possible to calculate inlet and outlet temperatures for all three heat exchangers, as well as the thermal power absorbed by the water in the heat recovery heat exchanger, called recovered

Table 1
Pressure drop in system components, according to [23].

System component	Pressure drop [kPa]
Air filter	1
Heat exchangers (hot and cold sides)	10
After-burner	2
SOFC (fuel side)	2
SOFC (oxidant side)	3
Pipes and elbows	0.5

thermal power and represented by Q_{rec} . This is the thermal power that the system supplies to an external user.

The heat exchangers' efficiency can be expressed as the ratio between the thermal power actually transferred from hot to cold fluid and the maximum thermal power that could be transferred:

$$\varepsilon_{\text{ex}} = \frac{c_{p,h}(T_{h,i}) \cdot T_{h,i} - c_{p,h}(T_{h,o}) \cdot T_{h,o}}{c_{p,h}(T_{h,i}) \cdot T_{h,i} - c_{p,h}(T_{c,i}) \cdot T_{c,i}} \quad (32)$$

3.5. Power electronics model

The power electronics' efficiency η_{PE} is considered constant even if the load varies, since the input voltage and current of the equipment are constant, and the efficiency variation of DC/DC and DC/AC devices between 20% and 100% of maximum power is typically lower than 3%. As a consequence, it is possible to calculate the net electric power available after the conversion by subtracting the power consumed by the auxiliary devices from the electric power generated by the SOFC, and multiplying the result by the power electronics' efficiency:

$$P_{\text{el}} = \eta_{\text{PE}} \cdot (P_{\text{el,SOFC}} - P_b - P_{\text{p,ethanol}} - P_{\text{p,water}}) \quad (33)$$

Using the net electric power it is also possible to determine the global electric efficiency of the system, defined as:

$$\eta_{\text{el}} = \frac{P_{\text{el}}}{P_{\text{tot}}} \quad (34)$$

4. Results and discussion

A computational simulation is made for the ensemble SOFC-BoP using the equations listed in Section 3 in order to evaluate the performance of different potential topologies for system construction, and to analyze the impact of the operational parameters on system behavior. Since the number of parameters is quite big, some of them are fixed at a constant value in order to limit the analysis to a few relevant situations. The values chosen for those parameters are listed in Table 2.

Besides these parameters, other variables are estimated either by using data from the literature, or by fixing them at conventional values. Table 3 shows these variables and their values.

In this section, an indicator called sensibility has been used to investigate the effect of a change in the operational parameters of the system on the electric efficiencies. The sensibility of the electric efficiency η_{el} to a change in the parameter p from a value $p^{(1)}$ to a value $p^{(2)}$ is defined as the ratio between the relative change in the efficiency and the relative change in p :

$$S_p = \frac{\frac{\eta_{\text{el}}^{(2)} - \eta_{\text{el}}^{(1)}}{\eta_{\text{el}}^{(1)}}}{\frac{p^{(2)} - p^{(1)}}{p^{(1)}}} \quad (35)$$

Table 2
Fixed parameter values.

Operational parameter	Value	Unit
Total electric power of the system	500	[W]
Single cell area	50	[cm ²]
Number of single cells	30	
SOFC inlet gas temperature	600	[°C]
SOFC internal temperature (solid components)	850	[°C]
System outlet gas temperature	80	[°C]
Inlet water temperature	25	[°C]
Outlet water temperature	45	[°C]

4.1. System supplied with pure ethanol

The stack receives a flow of pure ethanol in vapor form at the anode inlet. In the anodic compartments the fuel is decomposed into simpler substances, which take part in the electrochemical reactions. Ethanol decomposition happens through pyrolysis and steam reforming. It is assumed that the presence of water (product of the reactions), together with the materials used in the system's construction and the structure and management strategy of the BoP, prevent solid carbon deposition.

The main parameters that affect system operation are the λ ratios for ethanol ($\lambda_{\text{C}_2\text{H}_6\text{O}}$) and air (λ_{air}).

$$\lambda_{\text{C}_2\text{H}_6\text{O}} = \frac{\dot{n}_{\text{C}_2\text{H}_6\text{O}}}{\dot{n}_{\text{C}_2\text{H}_6\text{O,st}}} \quad (36)$$

$$\lambda_{\text{air}} = \frac{\dot{n}_{\text{air}}}{\dot{n}_{\text{air,st}}} \quad (37)$$

The numerator is the actual molar flow of ethanol or air, while the denominator is the minimum molar flow required to generate the desired current (st subscript).

System simulation was done using different $\lambda_{\text{C}_2\text{H}_6\text{O}}$ and λ_{air} values, obtaining Figs. 2–4. The efficiency values are calculated using ethanol's higher heating value. Figs. 2 and 3 show that an increase in $\lambda_{\text{C}_2\text{H}_6\text{O}}$, i.e. of fuel excess, causes a considerable drop in the electric efficiencies, both global and of the stack. In fact, the simulations are operated keeping P_{el} constant; therefore, an increase in $\lambda_{\text{C}_2\text{H}_6\text{O}}$ means that a higher fuel flow is being used to produce the same level of electric power, resulting in lower electric efficiencies. The impact of an increase in $\lambda_{\text{C}_2\text{H}_6\text{O}}$ on the electric efficiencies is higher for low $\lambda_{\text{C}_2\text{H}_6\text{O}}$ values. Moreover, the effect is slightly stronger on the electric efficiency of the stack than on the global one. This last result can also be confirmed by calculating the sensitivity of the electric efficiencies to the changes in $\lambda_{\text{C}_2\text{H}_6\text{O}}$. In fact, the mean value of the sensitivity of η_{el} to the simulated changes in $\lambda_{\text{C}_2\text{H}_6\text{O}}$ is -0.426 , while the same quantity for $\eta_{\text{el,SOFC}}$ is equal to -0.448 . Both values are negative, meaning that an increase in $\lambda_{\text{C}_2\text{H}_6\text{O}}$ leads to a decrease in the electric efficiencies, but $\eta_{\text{el,SOFC}}$ appears more sensitive to the parameter change. Another consequence of an increase of $\lambda_{\text{C}_2\text{H}_6\text{O}}$ with P_{el} constant is that a higher share of the fuel energy content is converted to heat; therefore, the thermal efficiency of the system increases, as can be seen in Fig. 4. Also, when λ_{air} rises, it is possible to observe a limited increase in the electric efficiency of the stack and a drop in the global electric efficiency. This occurs because when λ_{air} rises two conflicting effects develop: the stack's electric efficiency increases due to the higher partial pressure of the air in the cathode; the blower's power consumption also grows, since higher λ_{air} implies a higher air flow. The first effect contributes to an increase in the power produced by

Table 3
Estimated variable values.

Variable	Value	Unit
Power electronics' efficiency	94	[%]
Blower's isentropic efficiency	70	[%]
Pumps' isentropic efficiency	70	[%]
Pressure drop in the cathodic line	47.5	[kPa]
Pressure drop in the anodic line	55	[kPa]
Ambient pressure	101.325	[kPa]
Ambient temperature	25	[°C]
Dispersed thermal power (SOFC and after-burner)	120	[W]
Dispersed thermal power (air pre-heater)	80	[W]
Dispersed thermal power (fuel pre-heater)	80	[W]
Dispersed thermal power (heat recovery heat exchanger)	50	[W]

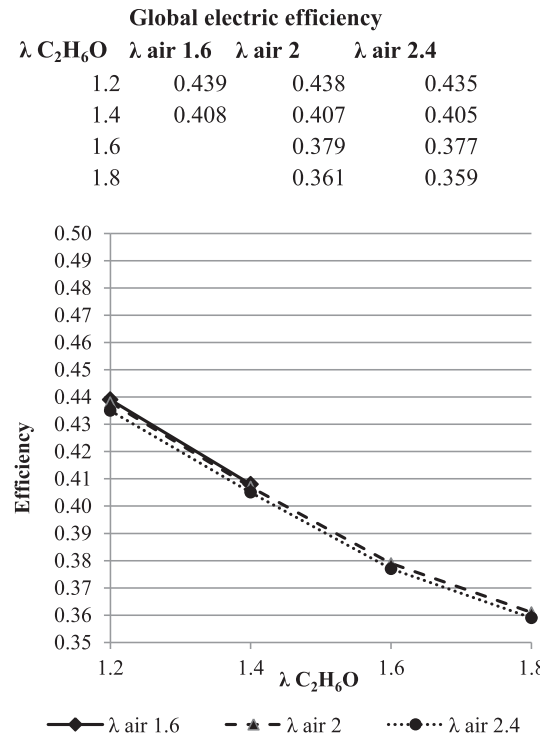


Fig. 2. Global electric efficiency as a function of $\lambda_{C_2H_6O}$. The graph shows three different trends in the global electric efficiency, each one corresponding to a different value of λ_{air} .

the stack for a constant fuel flow, while the second implies higher power consumption by the auxiliary devices. However, the second effect is more relevant than the first, resulting in a drop in the net electric power produced by the system and, therefore, in the global

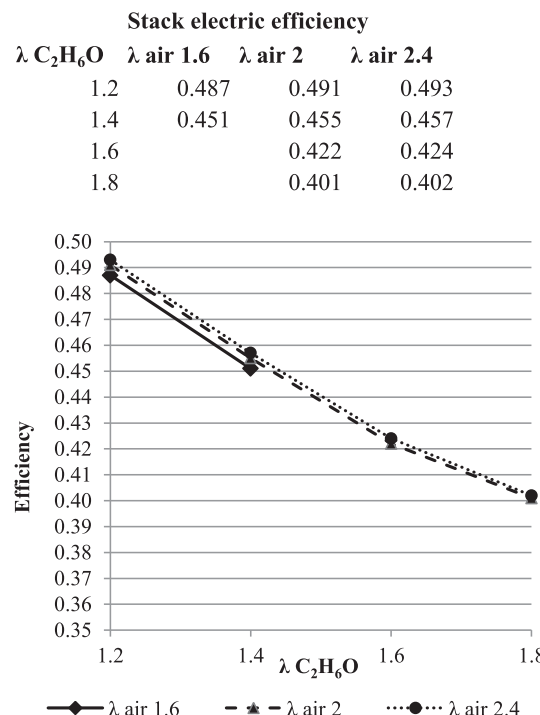


Fig. 3. Stack electric efficiency as a function of $\lambda_{C_2H_6O}$. The graph shows three different trends in the stack electric efficiency, each one corresponding to a different value of λ_{air} .

electric efficiency. Compared to $\lambda_{C_2H_6O}$, λ_{air} influences the system performance in a much smaller way, especially in simulations operated with high $\lambda_{C_2H_6O}$ values. The mean value of the sensitivity of η_{el} to the simulated changes in λ_{air} is -0.018 , meaning that an increase in λ_{air} leads to a much smaller decrease in η_{el} than the one observed in the case of an increase in $\lambda_{C_2H_6O}$.

According to the analysis conducted above, in order to maximize the electric efficiency, it is necessary to reduce $\lambda_{C_2H_6O}$ as much as possible. The lowest value of $\lambda_{C_2H_6O}$ that it will be possible to use in the real system mainly depends on the actual constructive characteristics of the stack. $\lambda_{C_2H_6O}$ values lower than 1.2 are not considered in the simulations, because below this threshold the risk of a fuel shortage for the electrochemical reactions would be substantial. In fact, the reactions that happen in the cells are never ideal, and therefore it is always necessary to ensure some fuel excess to be sure that the stack is able to sustain the desired current. Furthermore, a minimal difference of 0.2 between $\lambda_{C_2H_6O}$ and λ_{air} is maintained, in order to guarantee complete fuel combustion inside the after-burner. In fact, a smaller air/fuel ratio could result in the emission of uncombusted hydrocarbons from the system outlet.

4.2. System supplied with ethanol and water

Solid carbon deposition inside the SOFC and the pipes is an important problem for SOFC-based electric generation systems. To avoid it, the fuel is often supplied to the system with a certain amount of water. The necessary amount of water changes with the system characteristics. The parameter used to define this amount is the ratio between steam and ethanol molar flows, S/E .

$$\frac{S}{E} = \frac{\dot{n}_{H_2O}}{\dot{n}_{C_2H_6O}} \quad (38)$$

Values normally presented in the literature or used in prototype operation are between 2 and 5. Fig. 5 shows the effect of an increase

Global thermal efficiency

$\lambda_{C_2H_6O}$	$\lambda_{air\ 1.6}$	$\lambda_{air\ 2}$	$\lambda_{air\ 2.4}$
1.2	0.13	0.125	0.123
1.4	0.187	0.182	0.181
1.6		0.235	0.233
1.8		0.269	0.268

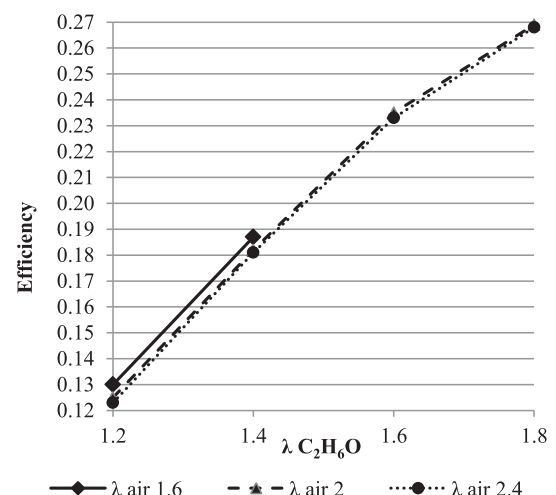


Fig. 4. Global thermal efficiency as a function of $\lambda_{C_2H_6O}$. The graph shows three different trends in the global thermal efficiency, each one corresponding to a different value of λ_{air} .

in the S/E value on both the global and the stack's electric efficiencies.

The graph is plotted using the couple of values of $\lambda_{C_2H_6O}$ and λ_{air} that generates the highest electric efficiency for the case of pure ethanol, and under the assumption that a pump is used to send the water flow to the stack. Fig. 5 clearly shows that the dilution of ethanol with water results in a drop in the global and stack's electric efficiencies. The drop in the global efficiency is mainly caused by the drop in the electric efficiency of the stack, but there is also a very limited additional deleterious effect, which is the power consumed by the pump. The more diluted the ethanol, the greater the loss in efficiency. With the lowest value of S/E used, the difference between efficiencies in the cases of pure and diluted ethanol is found to be equal to 2.8%. This difference increases as the value of S/E grows. This is reflected also by the values of the sensitivity of η_{el} to the changes in S/E : the mean of the sensitivity values calculated for the simulated steps of S/E is -0.058 , meaning that an increase in S/E causes a drop in η_{el} . This drop is smaller than the one caused by an increase in $\lambda_{C_2H_6O}$ and bigger than the one caused by an increase in λ_{air} , as can be noted by comparing the sensitivities calculated for $\lambda_{C_2H_6O}$, λ_{air} and S/E . Moreover, the sensitivity increases when the considered S/E values increase, confirming that the pejorative effect of a rise in S/E gets stronger when S/E rises.

4.3. Anodic recirculation

One method that is used to increase the water concentration in the anode compartments, reducing the probability of solid carbon formation inside the stack, is the partial recycling of anode outlet

S/E	Stack electric efficiency	Global electric efficiency
2	0.458	0.411
2.5	0.453	0.407
3	0.449	0.403
3.5	0.444	0.399
4	0.441	0.395
4.5	0.437	0.392
5	0.434	0.389

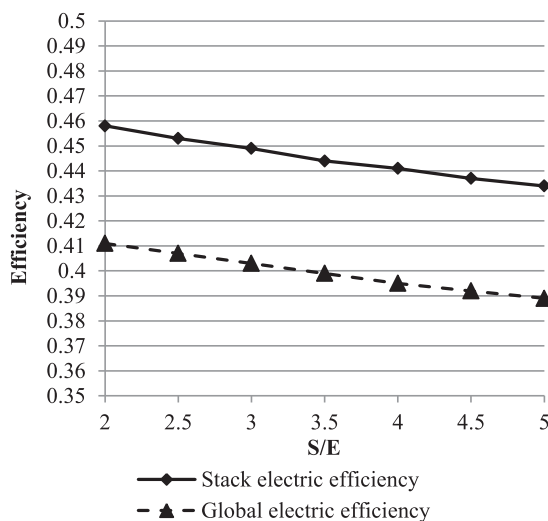


Fig. 5. Electric efficiencies, ethanol–water mixture. The trends of the stack electric efficiency and of the global electric efficiency as a function of S/E are reported for the case in which the system is fueled with an ethanol–water mixture, without the use of anodic recirculation.

gases to the anode inlet line. Through this mechanism, the steam produced in the electrochemical reactions is partially reintroduced into the stack, increasing the water concentration. This is often done using an ejector, which uses the pressure of the fresh fuel flow (supplied from outside the stack) to generate the recirculation flow. The parameter that fixes the degree of anodic recirculation is the fraction of the water flow introduced from outside the stack, i.e. the ratio between the water flow supplied with the fresh fuel and the total water flow that enters the anode (the sum of the flow coming from outside the stack and the flow resulting from gas recirculation):

$$f_{H_2O} = \frac{\dot{m}_{H_2O,out}}{\dot{m}_{H_2O}} \quad (39)$$

The lower this ratio, the greater the recirculation gas flow. System complexity is minimized when the stack's water demand is satisfied exclusively through gas recirculation, because in this case no water pump is necessary.

It is important to highlight that part of the fuel flow defined by $\lambda_{C_2H_6O}$ is contained in the recirculation gases: in fact, these gases contain non-oxidized fuel (in the present model, solely hydrogen, generated through ethanol decomposition in anodic compartments) that can still take part in the electrochemical reactions. This means that when using anodic recirculation an increase in fuel

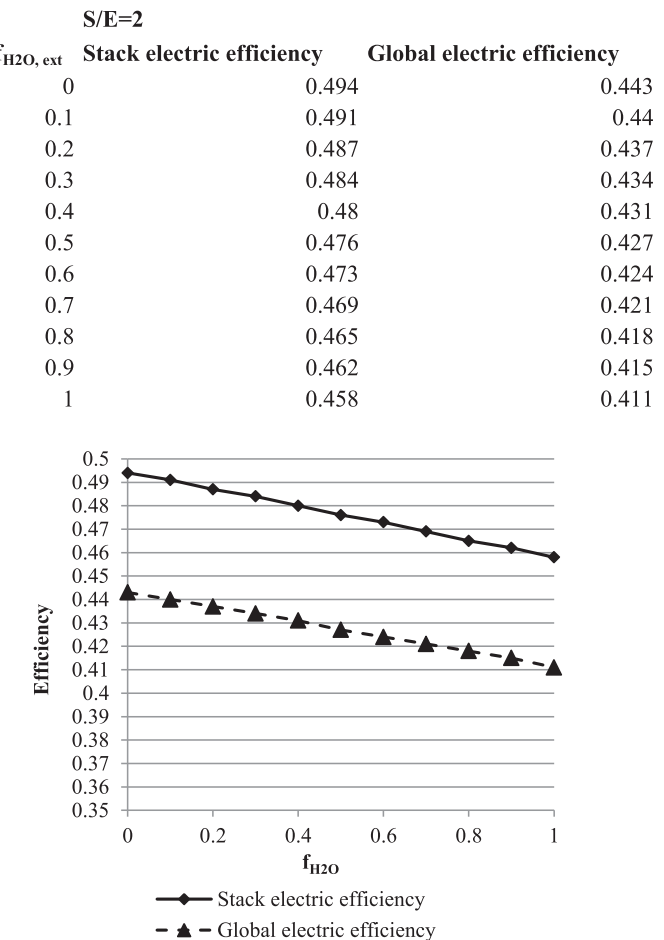


Fig. 6. Electric efficiencies, anodic recirculation, $S/E = 2$. The trends of stack's electric efficiency and of global electric efficiency as a function of f_{H_2O} are reported for the case in which the system is fueled with an ethanol–water mixture, using anodic recirculation and for a S/E value equal to 2.

excess is related to an increase in $n_{C_2H_6O}$ that is smaller than the one described in Subsections 4.1 and 4.2.

Figs. 6 and 7 show the electric efficiencies of the stack and the SOFC, for different values of f_{H_2O} and for S/E equal to 2 and 4. Comparing this data with the results displayed in Subsections 4.1 and 4.2, it can be concluded that with the use of anodic recirculation it is possible to obtain a high global electric efficiency, while maintaining S/E at the desired value. When S/E is equal to 2 (Fig. 6) and f_{H_2O} is lower than 0.2, the global electric efficiency is higher than with pure ethanol (Fig. 2), even though the difference is quite small (0.4% at the maximum).

As demonstrated in Subsection 4.2, an increase in S/E causes a global electric efficiency drop: when S/E is equal to 4 (Fig. 7), the global electric efficiency is the same as that observed for pure ethanol (Fig. 2) only when f_{H_2O} is 0. This means that for higher S/E values it is impossible to avoid a global electric efficiency drop with respect to the pure ethanol case, even using anodic recirculation.

By calculating the sensitivities of η_{el} to the steps of f_{H_2O} between the various simulations, it is possible to retrieve some additional information. The average of the sensitivities is -0.039 in the case of S/E equal to 2, while the same value is -0.054 for S/E equal to 4. This suggests that the influence of f_{H_2O} on η_{el} is bigger for high S/E values. Moreover, the absolute value of the sensitivity is higher when the considered values of f_{H_2O} are high. Therefore, the positive effects of anodic recirculation are very evident even with only small

reductions in the external water flow (i.e. f_{H_2O} close to 1), while the additional benefits are reduced when f_{H_2O} approaches 0 (at which point water is completely supplied through anodic recirculation). In this case, as in Subsection 4.2, the sensitivity of η_{el} to changes in f_{H_2O} proves lower than the sensitivity of η_{el} to changes in $\lambda_{C_2H_6O}$.

4.4. Cathodic recirculation

As with the anode, it is possible to recirculate part of the cathode outlet gases to the inlet of the cathodic compartments. In this case an ejector is often used. The cathodic recirculation reduces the compressed air flow required to obtain a given value of λ_{air} : this reduces the thermal energy required to pre-heat the air and the power consumption of the blower. As a consequence, when using this solution the auxiliary devices power consumption drops and the system's thermal performance improves.

In this case, the parameter that characterizes system operation is the cathodic recirculation fraction, defined as the ratio between recirculated gas flow and total cathode outlet flow.

$$f_{REC,C} = \frac{\dot{n}_{rec,C}}{\dot{n}_{out,C}} \quad (40)$$

An increase of $f_{REC,C}$ results in a reduction of oxygen concentration in the gas mixture that enters the cathodes, while the nitrogen content of the same mixture increases. Therefore, $f_{REC,C}$ can assume only those values that allow for a minimum flow of oxygen to sustain the reactions in the SOFC and in the after-burner.

Fig. 8 shows the effect of changes in $f_{REC,C}$: as expected, the increase in $f_{REC,C}$ causes a decrease in blower power consumption and an increase in recovered thermal power (due to a decrease in the thermal power required to pre-heat the air). The cathodic recirculation therefore reduces the electric consumption of the auxiliary devices, while improving the thermal management of the system

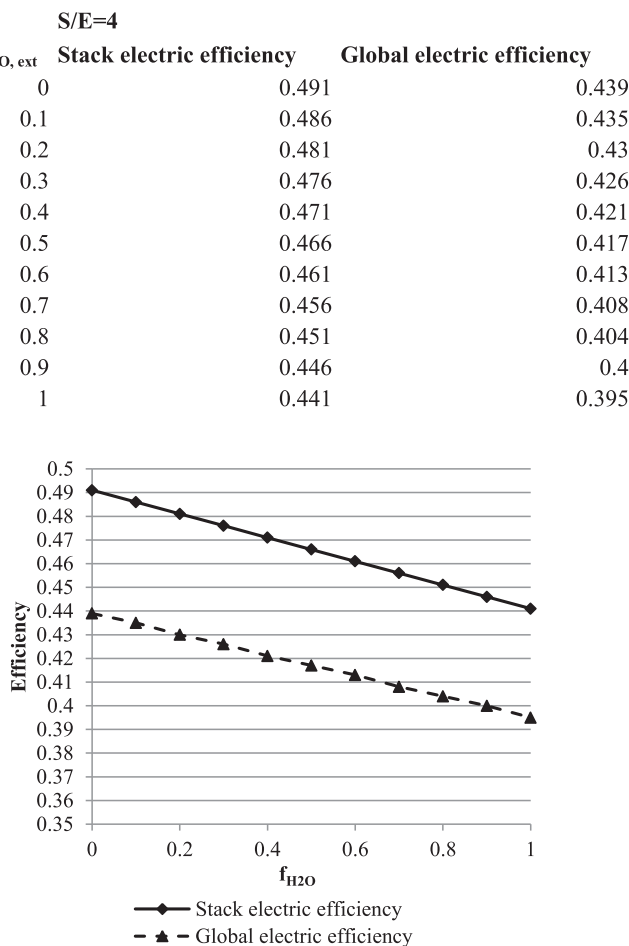


Fig. 7. Electric efficiencies, anodic recirculation $S/E = 4$. The trends of stack's electric efficiency and of global electric efficiency as a function of f_{H_2O} are reported for the case in which the system is fueled with an ethanol–water mixture, using anodic recirculation and for an S/E value equal to 4.

$f_{REC,C}$	Power consumed by the blower	Recovered thermal power
0	23.154	148.77
0.05	22.727	149.712
0.1	22.302	150.743
0.15	21.879	151.906
0.2	21.458	153.186
0.25	21.04	154.629
0.3	20.625	156.233

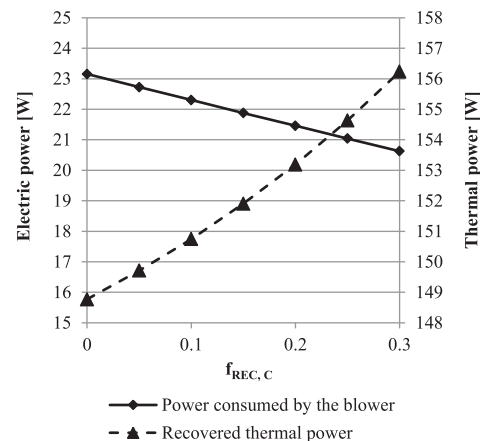


Fig. 8. Electric power consumed by the blower and recovered thermal power using cathodic recirculation. For the case in which the system employs the cathodic recirculation, trends of the electric power consumed by the blower and the recovered thermal power as a function of $f_{REC,C}$ are reported.

$f_{REC,C}$	Stack electric efficiency	Global electric efficiency	Global thermal efficiency
0	0.487	0.439	0.13
0.05	0.486	0.438	0.131
0.1	0.486	0.438	0.132
0.15	0.485	0.438	0.133
0.2	0.484	0.438	0.134
0.25	0.484	0.437	0.135
0.3	0.483	0.437	0.137

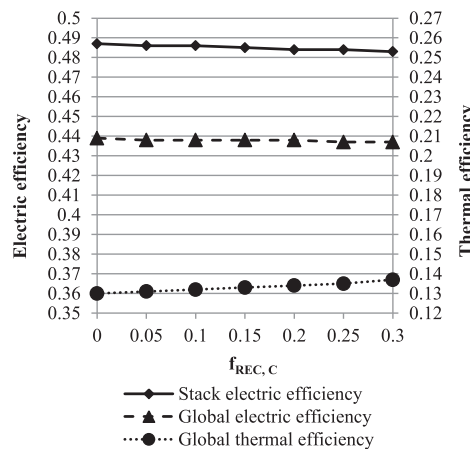


Fig. 9. Cathodic recirculation: stack electric efficiency, global electric efficiency and global thermal efficiency. The trends of stack's electric efficiency, of global electric efficiency and of global thermal efficiency as a function of $f_{REC,C}$ are shown for the case of cathodic recirculation.

and consequently the global thermal efficiency. Fig. 9 shows the behavior of the stack's electric efficiency, of the global electric efficiency and of the global thermal efficiency using cathodic recirculation.

An increase in $f_{REC,C}$ causes a reduction in cathodic oxygen concentration and consequently a drop in stack electric efficiency. At the same time, there is a reduction in the energy consumption of the auxiliary devices. Both effects influence the global electric efficiency, but the drop in the electric efficiency of the stack dominates, resulting in a global electric efficiency drop when $f_{REC,C}$ increases. However, this drop in global electric efficiency is very small, around 0.2% change when comparing the cases of $f_{REC,C}$

respectively equal to 0 and 0.3. The size of the impact of $f_{REC,C}$ on η_{el} is so small that the corresponding sensitivities are almost 0 in every case. On the other hand, the effect of cathodic recirculation on the global thermal efficiency is stronger: the thermal performance of the systems increases by approximately 0.7% for the same change in $f_{REC,C}$.

These results show that cathodic recirculation is not appropriate for a system that prioritizes electric production, because it causes a global electric efficiency reduction. However, cathodic recirculation can be advantageous if global thermal efficiency is an important parameter, because it generates an increase in thermal efficiency that is higher than the decrease in global electric efficiency. Still,

Table 4

Comparison between best performing operating conditions, identified for each analyzed system configuration.

Variable	1	2	3	4	Unit
	Pure ethanol	Ethanol and water mixture	Pure ethanol with anodic recirculation	Pure ethanol with cathodic recirculation	
$\lambda_{C_2H_6O}$	1.2	1.2	1.2	1.2	
λ_{air}	1.6	1.6	1.6	1.6	
S/E	0	2	2	0	
$f_{REC,C}$	0	0	0	0.3	
f_{H_2O}	1	1	0	1	
Global electric efficiency	43.9	41.1	44.3	43.7	[%]
Global thermal efficiency	13	17.1	12	13.7	[%]
Ethanol flow rate	2.9	3.1	2.87	2.92	[ml min ⁻¹]
Fuel chemical power	1140	1215	1128	1144	[W]
SOFC DC electric power	555	557	558	553	[W]
Recovered thermal power	149	208	135	156	[W]
Power consumed by the ethanol pump	4	4	4	4	[mW]
Power consumed by the water pump	0	3	0	0	[mW]
Power consumed by the blower	23.2	24.7	25.7	20.6	[W]
Mean cell voltage	694	653	651	688	[mV]
Stack voltage	20.8	19.6	19.5	20.7	[V]
Stack current	26.7	28.4	28.5	26.8	[A]
After-burner outlet gas temperature	1026	1027	984	1067	[°C]

The global electric efficiencies reported in bold characters are related to the system configurations indicated as most convenient in Section 5.

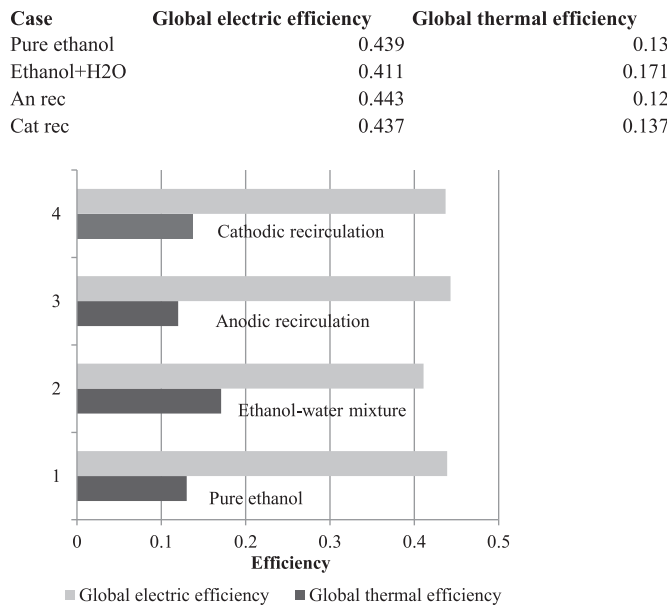


Fig. 10. Global system efficiencies, comparison. The highest values of global electric efficiency and global thermal efficiency obtained for each system configuration are reported.

this increase in global thermal efficiency is not very high; therefore, this beneficial effect would hardly legitimate the higher system complexity required for the application of cathodic recirculation.

4.5. Comparison

Table 4 shows the values of the variables analyzed, taking into account the different operational conditions considered in this study. The situations included in **Table 4** and **Figs. 10 and 11** are the ones that present the highest global electric efficiency for each configuration, except for the case of cathodic recirculation, where the situation of maximum total efficiency (sum of thermal and electric efficiencies) was reported. In **Fig. 10** it can be seen that the global electric efficiency shows its maximum value when anodic recirculation is adopted, and that the variation of this parameter

among all situations is quite small. The figure also shows an inverse relationship between electric efficiency and thermal efficiency. The cases characterized by higher global thermal efficiency also present higher values of recovered thermal power, as shown in **Fig. 11**. This figure also reports data about blower power consumption, which is approximately constant in all situations, except in case of cathodic recirculation, when the value is lower. Also stack's electric power varies in a limited manner among the reported cases.

The analysis of the system behavior when the various parameters change provides information about their desirable values. In general, in order to maximize the global electric efficiency of the system it is good to work with low $\lambda_{C_2H_6O}$ and λ_{air} values and to set $f_{REC,C}$ equal to 0 (i.e. not to use cathodic recirculation). If the characteristics of the system impose a water flow to the anode together with the fuel to avoid solid carbon deposition (i.e. a S/E value higher than 0), it is desirable to use values of S/E and f_{H_2O} as low as possible. Comparing the average sensitivities of η_{el} to a change in the various parameters, it is possible to conclude that the most influential parameter is $\lambda_{C_2H_6O}$, followed by S/E and f_{H_2O} , this last one especially in the case of high S/E values. λ_{air} and $f_{REC,C}$ are characterized instead by a limited effect, almost nonexistent in the case of $f_{REC,C}$.

5. Conclusions

The analysis of the simulation results with pure ethanol, shown in **Figs. 2–4** and reported in **Table 4**, leads to the conclusion that an increase in fuel excess, i.e. a higher value of $\lambda_{C_2H_6O}$, causes a substantial reduction in the global electric efficiency and an increase in the thermal efficiency. **Fig. 5** clearly shows that ethanol dilution with water causes a considerable drop in system efficiency if water is supplied by a dedicated pump. The effect on the efficiency of the system is less negative, or even positive, if water concentration is increased by partial recirculation of anode outlet gases. The recirculation of cathode outlet gases has a more limited effect, which is therefore not interesting for the considered application.

Table 4 summarizes the values of the variables that were obtained during the simulations. All the efficiency values reported in the table are related to ethanol's higher heating value. The results show that there are two convenient system configurations:

- Operation with pure ethanol, without recirculation

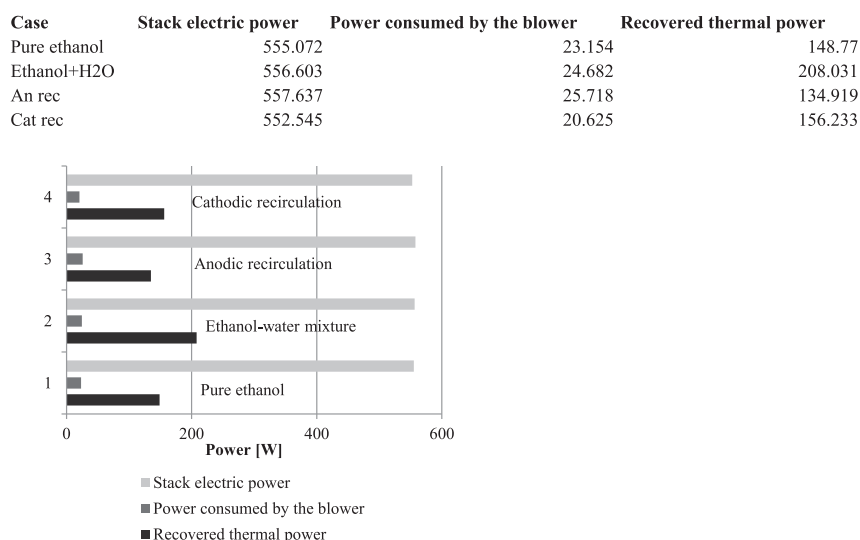


Fig. 11. System power, comparison. The values of stack's electric power, blower power consumption and recovered thermal power, obtained for the same system configurations considered in **Fig. 10**, are reported.

In this case the system is very simple, since it does not require injectors or a water pump. At the same time, the global electric efficiency is high (43.9%). However, system operation in this case requires the use of suitable materials and an appropriate BoP structure and management, to prevent solid carbon deposition.

- Operation with partial recirculation of anodic reaction products

In this configuration the system is more complex, even if it does not require a water pump, but there is a lower probability of solid carbon deposition. Moreover, the global electric efficiency is slightly higher than the one observed when operating with pure ethanol without recirculation (44.3%).

Finally, these results suggest that the most convenient solution for this project is a pure ethanol operation without recirculation, made possible by the use of proprietary anode components ([15,16]), which were developed especially to avoid solid carbon formation. As a consequence, the data from this pure ethanol simulation will be used as a reference to fix a tentative operating point for the system and to continue with the prototype project, as established in the research plan. In the continuation of the prototype development, economic considerations about the cost of the system will be included in the decision process.

As stated in the introduction, the efficiency of fuel cell based electricity generation systems is approximately constant for a wide range of system's nominal power. This means that, in the future, it would be possible to easily extend these results to other power levels, implementing electric generation systems characterized by higher powers.

Acknowledgments

This paper was developed under the Research and Technological Development Program of the Electric Energy Department regulated by the Brazilian Federal Energy Regulatory Agency (ANEEL), with the support of Elektro company. This paper was also partially supported by the Superior Level Personnel Improvement Coordination (CAPES).

References

- [1] J. Larminie, A. Dicks, *Fuel Cell Systems Explained*, second ed., Wiley, Chichester, 2003.
- [2] AEA, Harwell, *Combined Heat and Power Background*, European Commission - DG Environment, 2010.
- [3] A. Thornton, C. Rodríguez Monroy, *Renew. Sustain. Energy Rev.* 15 (2011) 4809–4817.
- [4] A. Elgowainy, L. Gaines, M. Wang, *Int. J. Hydrogen Energy* 34 (2009) 3557–3570.
- [5] *Fuel Cells Bull.* 2012 6 (2012) 5–6.
- [6] *Fuel Cells Bull.* 2012 10 (2012) 4.
- [7] Balanço energético nacional 2012, Energy Research Company (Empresa de Pesquisa Energética – EPE) and Brazilian Mines and Energy Department (Ministério de Minas e Energia do Brasil – MME), EPE, Rio de Janeiro, 2012.
- [8] <http://www.brasil.gov.br/infograficos/luz-para-todos-beneficiados>, (last accessed on 01.09.13).
- [9] G. Richter, Lecture at Rio de Janeiro Commerce Association (ACRJ) Seminar “Autoprodução de Energia Elétrica na Ponta”, 08/08/2012.
- [10] Projeção da demanda de energia elétrica para os próximos 10 anos (2013–2022), Energy Research Company (EPE – Empresa de Pesquisa Energética) and Brazilian Mines and Energy Department (MME - Ministério de Minas e Energia do Brasil), EPE, Rio de Janeiro, 2012.
- [11] ANEEL Technical Note nº 128/2011-SRT-SCT-SFF/ANEEL.
- [12] M. Demarty, J. Bastien, *Energy Policy* 39 (2011) 4197–4206.
- [13] A.C.C. de Souza, *Renew. Sustain. Energy Rev.* 12 (2008) 1843–1863.
- [14] S.O.A. Torres, A.C. Mesquita Filho, P.E.V. Miranda, *IEEE Lat. Am. Trans.* 11 (2) (2013).
- [15] A. Nakajo, F. Mueller, J. Brouwer, J. Van Herle, D. Favrat, *Int. J. Hydrog. Energy* 37 (2012) 9269–9286.
- [16] P.E.V. de Miranda, S.A. Venâncio, H.V. de Miranda, INPI Patenting Process nº PI0901921-9A2, 2009.
- [17] S.A. Venâncio, P.E.V. de Miranda, *Scr. Mater.* 65 (2011) 1065–1068.
- [18] S.L. Douvartzides, F.A. Coutelieris, P.E. Tsiakaras, *J. Power Sources* 114 (2003) 203–212.
- [19] Wen-Tang Hong, Tzu-Hsiang Yen, Tsang-Dong Chung, Cheng-Nan Huang, Bao-Dong Chen, *Appl. Energy* 88 (2011) 3990–3998.
- [20] M. Cimenti, J. M. Hill, *Energies* 2, 377–410.
- [21] P. Leone, A. Lanzini, G.A. Ortigoza-Villalba, R. Borchellini, *Chem. Eng. J.* 191 (2012) 349–355.
- [22] S.D. Nobrega, M.V. Galesco, K. Girona, D.Z. de Florio, M.C. Steil, S. Georges, F.C. Fonseca, *J. Power Sources* 213 (2012) 156–159.
- [23] R.J. Braun, *Optimal Design and Operation of Solid Oxide Fuel Cell Systems for Small Scale Stationary Applications*, Department of Mechanical Engineering, University of Wisconsin Madison, Madison, 2002 (PhD. thesis).
- [24] S.A. Hajimolana, M.A. Hussain, W.M.A. Wan Daud, M. Soroudi, A. Shamiri, *Renew. Sustainable Energy Rev.* 15 (2011) 1893–1917.